

# *Chapter 6*

**DIELECTRIC RELAXATION  
PHENOMENA AND HIGH  
FREQUENCY CONDUCTIVITY OF  
RIGID POLAR LIQUIDS IN  
DIFFERENT SOLVENTS**

# DIELECTRIC RELAXATION PHENOMENA AND HIGH FREQUENCY CONDUCTIVITY OF RIGID POLAR LIQUIDS IN DIFFERENT SOLVENTS

## 1. INTRODUCTION

Dielectric relaxation studies of polar liquids in nonpolar solvents are of much importance as they provide interesting information on solute-solvent and solute-solute molecular formations [1-2] under high frequency (hf) electric field. In order to predict associational aspects of polar liquids one must analyze the measured relaxation parameters to know the relaxation time  $\tau$  and the dipole moment  $\mu$  of a polar liquid by Cole-Cole [3], Cole-Davidson [4] plots or by single frequency concentration variation method [5].

Srivastava and Srivastava [6] studied the relaxation behaviour of chloral and ethyl trichloroacetate in different nonpolar solvents under various hf electric fields from the measured relaxation permittivities like real  $\epsilon'_{ij}$  and imaginary  $\epsilon''_{ij}$ , static  $\epsilon_{oij}$  and infinite frequency permittivity  $\epsilon_{\infty ij}$  of polar solute (j) in different nonpolar solvents (i) at 30°C to predict the solute-solvent or solute-solute associations in them. They, however, inferred that such molecules may possess two or more relaxation processes towards dielectric dispersion phenomena [6]. The molecule chloral is widely used in medicine and in the manufacture of D.D.T. as insecticide. Ethyl trichloroacetate, on the other hand, is used for artificial fragrance of fruits and flowers.

All these facts inspired us to use the measured relaxation data [6] for such polar liquids only to detect the double relaxation times  $\tau_1$  and  $\tau_2$  due to rotations of their flexible parts and the whole molecules themselves from the single frequency measurement technique [7-8]. Earlier investigations have been made on different chain like polar molecules like alcohols in a nonpolar solvent [9-10] to see the double relaxation phenomena at three different electric field

frequencies. However, no such study is made on such rigid aliphatic polar liquids in different nonpolar solvents under various electric field frequencies by the double relaxation theory based on single frequency measurements of dielectric relaxation parameters [7-8]. Moreover, their measured permittivities [6] have dimensions. It is, therefore, better to replace them in terms of dimensionless dielectric constants in SI units because of its rationalised and unified nature.

Five systems out of twelve as presented in table 1 show the double relaxation times  $\tau_2$  and  $\tau_1$ . The values of  $\tau_2$  and  $\tau_1$  were calculated from the slope and intercept of the linear equation (7) (see later). All the straight lines are shown graphically in figure 1.

The dipole moments  $\mu_2$  and  $\mu_1$  of Table 2 due to  $\tau_2$  and  $\tau_1$  were also calculated in terms of slopes  $\beta$ 's of total hf conductivity  $\sigma_{ij}$  against  $w_j$  curves. The  $\sigma_{ij}$ - $w_j$  curves are displayed in figure 2. All the slight parabolic curves of conductivities with  $w_j$  are found to increase with frequency of the electric field. The calculated  $\mu$ 's are compared with the theoretical dipole moment  $\mu_{\text{theo}}$  due to available bond angles and bond moments which are sketched in figure 3 showing the associational aspect of the polar molecules with solvents to observe the mesomeric and inductive moments in them under hf electric field. They are finally compared with the reported  $\mu$ 's and  $\mu_1$  obtained from  $\mu_1 = \mu_2(c_1/c_2)^{1/2}$  assuming two relaxation processes are equally probable.

The relative contributions  $c_1$  and  $c_2$  towards dielectric dispersions for the five systems were obtained from the theoretical values of  $x = (k'_{ij} - k_{\infty ij}) / (k_{oij} - k_{\infty ij})$  and  $y = k''_{ij} / (k_{oij} - k_{\infty ij})$  of Fröhlich's theory [11] in terms of estimated  $\tau_2$  and  $\tau_1$  of Table 1. They were also computed from the values of  $x$  and  $y$  at  $w_j \rightarrow 0$  of graphical technique [7-8] and placed in table 3 for comparison with Fröhlich's  $c_1$  and  $c_2$ . The variations of  $x$  and  $y$  with  $w_j$  of solute of figures 4 and 5 are the least square fitted parabolae with the experimental data. They are of convex and concave shapes except ethyl trichloroacetate in n-hexane at 9.8 and 24.6 GHz electric fields. This sort of behaviours was not observed earlier [7-8]. With these values of  $x$  and  $y$  at  $w_j \rightarrow 0$  the symmetric and asymmetric distribution parameters  $\gamma$

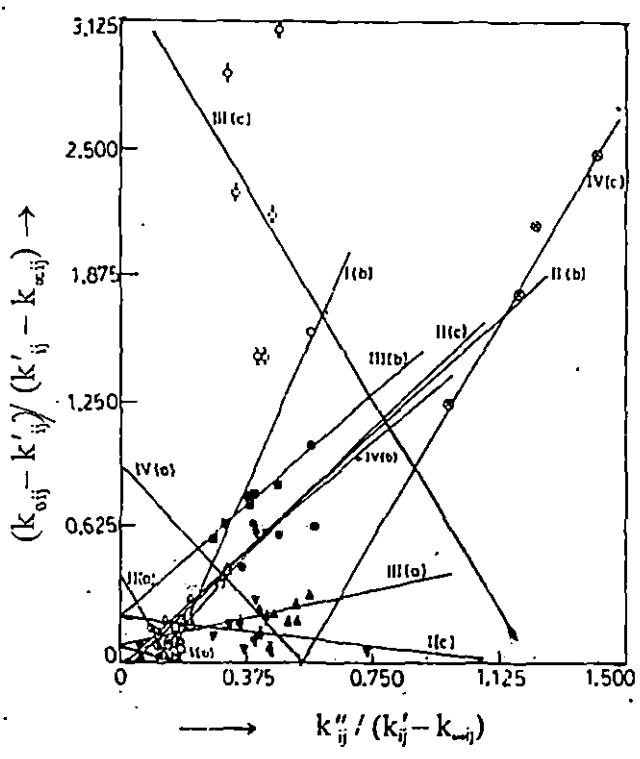


Figure 1 : Linear variation of  $(k_{0ij} - k'_{ij}) / (k'_{ij} - k_{\infty ij})$  against  $k''_{ij} / (k'_{ij} - k_{\infty ij})$  for different  $w_j$ 's of chloral and ethyltrichloroacetate under three different hf electric fields at 30°C. I(a), I(b) and I(c) for chloral in benzene ( $\times$ ,  $\circ$ ,  $\nabla$ ); II(a), II(b) and II(c) for chloral in n-heptane ( $\bullet$ ,  $\Delta$ ,  $\square$ ); III(a), III(b) and III(c) for ethyltrichloroacetate in benzene ( $\blacktriangle$ ,  $\blacksquare$ ,  $\diamond$ ) and IV(a), IV(b) and IV(c) for ethyltrichloroacetate in n-hexane ( $\blacklozenge$ ,  $\bullet$ ,  $\oplus$ ) at 4.2, 9.8 and 24.6 GHz electric fields respectively.

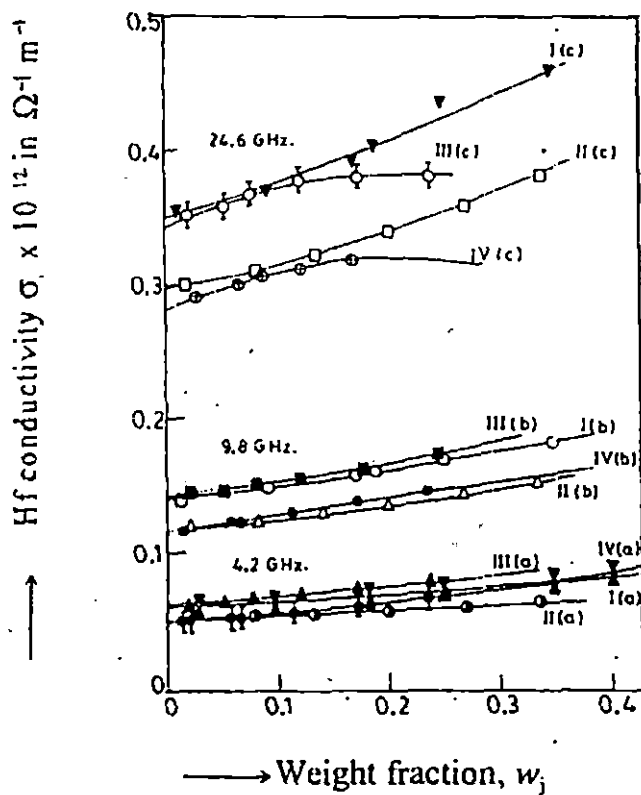


Figure 2 : Hf conductivity  $\sigma$ ,  $\times 10^{12}$  in  $\Omega^{-1} \text{ m}^{-1}$  against  $w_1$  of solutes at  $30^\circ\text{C}$ . I(a), I(b) and I(c) for chloral in benzene ( $\nabla$ ,  $\circ$ ,  $\blacktriangledown$ ); II(a), II(b) and II(c) for chloral in n-heptane ( $\bullet$ ,  $\triangle$ ,  $\square$ ); III(a), III(b) and III(c) for ethyltrichloroacetate in benzene ( $\blacktriangle$ ,  $\blacksquare$ ,  $\diamond$ ) and IV(a), IV(b) and IV(c) for ethyltrichloroacetate in n-hexane ( $\blacklozenge$ ,  $\bullet$ ,  $\oplus$ ) at 4.2, 9.8 and 24.6 GHz electric fields respectively.

and  $\delta$  of the molecules at those frequencies are computed and are placed in table 3 to indicate the nonrigidity of the molecules in hf electric field.

## 2. THEORETICAL FORMULATIONS

Assuming the molecules to possess two separate broad dispersions under hf electric field, Bergmann equations [12] are :

$$\frac{\epsilon'_{ij} - \epsilon_{\infty ij}}{\epsilon_{oij} - \epsilon_{\infty ij}} = \frac{c_1}{1 + \omega^2 \tau_1^2} + \frac{c_2}{1 + \omega^2 \tau_2^2} \quad \dots\dots\dots (1)$$

$$\frac{\epsilon''_{ij}}{\epsilon_{oij} - \epsilon_{\infty ij}} = c_1 \frac{\omega \tau_1}{1 + \omega^2 \tau_1^2} + c_2 \frac{\omega \tau_2}{1 + \omega^2 \tau_2^2} \quad \dots\dots\dots (2)$$

such that the sum of the relative weight factors  $c_1$  and  $c_2$  towards dielectric dispersion is unity i.e.  $c_1 + c_2 = 1$ .

When the dielectric relaxation permittivities in equations (1) and (2) are expressed in terms of internationally accepted symbols like real  $k'_{ij}$  ( $= \epsilon'_{ij} / \epsilon_o$ ), imaginary  $k''_{ij}$  ( $= \epsilon''_{ij} / \epsilon_o$ ) parts of complex dimensionless dielectric constant  $k^*_{ij}$ , static  $k_{oij}$  ( $= \epsilon_{oij} / \epsilon_o$ ) and infinite frequency dielectric constant  $k_{\infty ij}$  ( $= \epsilon_{\infty ij} / \epsilon_o$ ) where  $\epsilon_o =$  permittivity of free space  $= 8.854 \times 10^{-12}$  F.m<sup>-1</sup>, the Bergmann equations (1) and (2) are given by :

$$\frac{k'_{ij} - k_{\infty ij}}{k_{oij} - k_{\infty ij}} = \frac{c_1}{1 + \omega^2 \tau_1^2} + \frac{c_2}{1 + \omega^2 \tau_2^2} \quad \dots\dots\dots (3)$$

$$\frac{k''_{ij}}{k_{oij} - k_{\infty ij}} = c_1 \frac{\omega \tau_1}{1 + \omega^2 \tau_1^2} + c_2 \frac{\omega \tau_2}{1 + \omega^2 \tau_2^2} \quad \dots\dots\dots (4)$$

Solving equations (3) and (4) for  $c_1$  and  $c_2$  one gets,

$$c_1 = \frac{(\alpha_2 - y)(1 + \alpha_1^2)}{\alpha_2 - \alpha_1} \quad \dots\dots\dots (5)$$

$$c_2 = \frac{(y - x\alpha_1)(1 + \alpha_2^2)}{\alpha_2 - \alpha_1} \dots\dots\dots (6)$$

where  $x = (k'_{ij} - k_{\infty ij}) / (k_{oij} - k_{\infty ij})$  and  $y = k'' / (k_{oij} - k_{\infty ij})$ . The term  $\alpha = \omega\tau$  and suffices 1 and 2 are, however, related to  $\tau_1$  and  $\tau_2$  respectively.

Adding equations (5) and (6) one gets :

$$\frac{k_{oij} - k'_{ij}}{k'_{ij} - k_{\infty ij}} = \omega (\tau_1 + \tau_2) \frac{k''_{ij}}{k'_{ij} - k_{\infty ij}} - \omega^2 \tau_1 \tau_2, \dots\dots\dots (7)$$

which is a linear equation having intercept-  $\omega^2 \tau_1 \tau_2$  and slope  $\omega(\tau_1 + \tau_2)$ . They are obtained from the measured dielectric constants at different  $\omega$ 's of solutes under a single frequency electric field  $\omega (= 2\pi f, f$  being the frequency in GHz) at a given temperature by applying linear regression technique.

Assuming a single broad Debye like dispersion for the polar molecules the equation (7) is reduced to the form (8) with  $\tau_1 = 0$  :

$$\frac{k_{oij} - k'_{ij}}{k'_{ij} - k_{\infty ij}} = \omega\tau_2 \frac{k''_{ij}}{k'_{ij} - k_{\infty ij}} \dots\dots\dots (8)$$

in order to get  $\tau_2$  for seven polar-non-polar liquid mixtures of table 1. The data thus obtained are placed in the 11th column of Table 1.

Again, the complex hf conductivity  $\sigma_{ij}^*$  is related to  $k'_{ij}$  and  $k''_{ij}$  by the relation:

$$\sigma_{ij}^* = \sigma'_{ij} + j\sigma''_{ij}$$

where  $\sigma'_{ij} = \omega\epsilon_0 k''_{ij}$  and  $\sigma''_{ij} = \omega\epsilon_0 k'_{ij}$  are the real and imaginary parts of the complex conductivity.

The magnitude of total hf conductivity is given by :

$$\sigma_{ij} = \omega\epsilon_0 \sqrt{k''_{ij}{}^2 + k'_{ij}{}^2} \dots\dots\dots (9)$$

**Table - 1.** The estimated relaxation time  $\tau_2$  and  $\tau_1$  from the slopes and the intercepts of straight line Equ (7) with % of errors and correlation coefficients (r) together with measured  $\tau_s$  from  $\sigma''_{ij} - \sigma'_{ij}$  curve and  $\tau$ 's from single broad dispersion for apparently rigid aliphatic molecules at 30°C under different frequencies of electric fields.

System with Sl. No. and mol wt, $M_1$ in Kg.	Frequency in GHz (f)	Intercept & slope of Equation (7) m c		Correlation coefficient (r)	% of error in regres- sion tech- nique	Estimated Values of $\tau_2$ & $\tau_1$ in psec		Measured $\tau_s$ in psec	Reported $\tau$ in psec	$\tau_s$ 's in psec from single broad dispersion of equ. (8)
(I) chloral in benzene $M_1 = 0.1475$ kg.	(a) 4.2	- 0.3872	- 0.0732	- 0.91	5.54	5.27	-	4.77	-	4.78
	(b) 9.8	3.7238	0.5497	0.99	0.09	57.98	2.50	2.36	1.78*	-
	(c) 24.6	- 0.1936	- 0.2161	- 0.41	25.08	2.45	-	1.73	-	2.01
(II) chloral in in n-Heptane $M_1 = 0.1475$ Kg.	(a) 4.2	- 2.7611	- 0.4191	- 0.78	12.81	5.44	-	3.74	-	40.87
	(b) 9.8	1.6593	0.1040	0.93	3.89	25.89	1.06	1.82	0.46*	-
	(c) 24.6	1.7458	0.1752	0.95	2.56	10.60	0.69	0.91	-	-
(III) ethyl trichloroacetate in benzene $M_1 = 0.1915$ Kg.	(a) 4.2	0.3545	- 0.0699	0.37	23.75	18.78	-	23.00	-	18.71
	(b) 9.8	1.5123	- 0.1797	0.96	1.87	26.36	-	7.28	6.5**	32.53
	(c) 24.6	- 2.7470	- 3.3227	- 0.24	25.86	5.88	-	3.34	-	37.19
(IV) ethyl trichloracetate in n-hexane $M_1 = 0.1915$ Kg.	(a) 4.2	- 1.7251	- 0.9325	- 0.26	25.68	16.38	-	16.53	-	20.13
	(b) 9.8	1.5182	0.0549	0.66	15.40	24.05	0.60	6.28	5.7**	-
	(c) 24.6	2.9891	1.6141	0.98	0.83	14.76	4.58	5.76	-	-

\* Cole-Cole Plot.

\*\* Gopala Krishna's Method

$\sigma''_{ij}$  is related to  $\sigma'_{ij}$  by the relation :

$$\sigma''_{ij} = \sigma_{\alpha ij} + \frac{1}{\omega\tau_s} \sigma'_{ij} \quad \dots\dots\dots(10)$$

where  $\tau_s$  is the measured relaxation time of a polar unit and  $\sigma_{\alpha ij}$  is the constant conductivity at  $w_j \rightarrow 0$ .

In the hf region, total conductivity  $\sigma_{ij} \simeq \sigma'_{ij}$ , hence equation (10) is written as :

$$\text{or } \sigma_{ij} = \sigma_{\alpha ij} + \frac{1}{\omega\tau_s} \sigma'_{ij}$$

$$\text{or } \left( \frac{d\sigma_{ij}}{d\omega_j} \right)_{w_j \rightarrow 0} = \frac{1}{\omega\tau_s} \left( \frac{d\sigma'_{ij}}{d\omega_j} \right)_{w_j \rightarrow 0}$$

$$\text{or } \beta = \frac{1}{\omega\tau_s} \left( \frac{d\sigma_{ij}}{d\omega_j} \right)_{w_j \rightarrow 0} \quad \dots\dots\dots(11)$$

The real part of hf conductivity  $\sigma'_{ij}$  at T K for  $w_j$  of a solute is [13 - 14] :

$$\sigma'_{ij} = \frac{N\rho_{ij}\mu_{ij}^2}{27\epsilon_0 k_B T M_j} \left( \frac{\omega^2\tau}{1 + \omega^2\tau^2} \right) (\epsilon_0 k_{\alpha ij} + 2) (\epsilon_0 k_{\alpha ij} + 2) w_j \quad \dots\dots\dots(12)$$

On differentiation with respect to  $w_j$  and at  $w_j \rightarrow 0$  equation (12) becomes :

$$\left( \frac{d\sigma'_{ij}}{d\omega_j} \right)_{w_j \rightarrow 0} = \frac{N\rho_{ij}\mu_{ij}^2}{3\epsilon_0 k_B T M_j} \left( \frac{\epsilon_i + 2}{3} \right)^2 \left( \frac{\omega^2\tau}{1 + \omega^2\tau^2} \right) \quad \dots\dots\dots(13)$$

where all the symbols expressed in S I units carry usual meanings [14]. From equations (11) and (13) one gets  $\mu_j$  from :

$$\mu_j = \left( \frac{27\epsilon_0 k_B T M_j \beta}{N \rho_{ij} (\epsilon_i + 2)^2 \omega b} \right)^{1/2} \quad \dots\dots\dots(14)$$

The dimensionless parameter b is related to  $\tau$  by :

$$b = \frac{1}{1 + \omega^2 \tau^2} \quad \dots\dots\dots (15)$$

All the  $\mu_j$ 's,  $b$ 's and  $\beta$ 's as computed for chloral and ethyl trichloroacetate are placed in Table 2.

The molecules under consideration are of complex type and only a few data are available under single frequency measurement in the low concentration region. In this case a continuous distribution of  $\tau$ 's with two discrete values of  $\tau_1$  and  $\tau_2$  could be expected [12]. Thus from Fröhlich's theory [11] based on distribution of  $\tau$  between the two extreme values of  $\tau_1$  and  $\tau_2$  we get :

$$x = \frac{k'_{ij} - k_{\infty ij}}{k_{oij} - k_{\infty ij}} = 1 - \frac{1}{2A} \ln \left( \frac{1 + e^{2A} \omega^2 \tau_s^2}{1 + \omega^2 \tau_s^2} \right) \quad \dots\dots\dots (16)$$

$$y = \frac{k''_{ij}}{k_{oij} - k_{\infty ij}} = \frac{1}{A} [\tan^{-1}(e^A \omega \tau_s) - \tan^{-1}(\omega \tau_s)] \quad \dots\dots\dots (17)$$

where  $\tau_s$  = small limiting relaxation time =  $\tau_1$  and  $A$  = Fröhlich parameter =  $\ln(\tau_2/\tau_1)$ . The theoretical values of  $x$  and  $y$  of equations (16) and (17) were used to get  $c_1$  and  $c_2$ . The values of  $c_1$  and  $c_2$  can also be had from the graphical plots of  $x$  and  $y$  at  $\omega_j \rightarrow 0$  as seen in figures 4 and 5 respectively.  $c_1$  and  $c_2$  thus obtained by both the methods are placed in Table 3 for comparison.

The molecules under five different environments show double relaxation phenomena (Table 1) indicating their nonrigidity. In such cases dielectric relaxation behaviour may be represented by [3-4] :

$$\frac{k^*_{ij} - k_{\infty ij}}{k_{oij} - k_{\infty ij}} = \frac{1}{1 + (j\omega\tau_s)^{(1-\gamma)}} \quad \dots\dots\dots (18)$$

$$\text{and} \quad \frac{k^*_{ij} - k_{\infty ij}}{k_{oij} - k_{\infty ij}} = \frac{1}{(1 + j\omega\tau_{cs})^\delta} \quad \dots\dots\dots (19)$$

**Table - 2.** Estimated intercept and slope of  $\sigma_{ij} - w_i$  equations, dimensionless parameters  $b_2, b_1$  [equ.(15)], estimated dipole moments  $\mu_2, \mu_1$  'eqe (14),  $\mu_{theo}$  from bond angles and bond moments together with  $\mu_1$  from  $\mu_1 = \mu_2 (c_1/c_2)^{1/2}$  and reported  $\mu$  in Coulomb-metre.

System with Sl. No. and mol wt, $M_j$ in Kg.	Frequency In GHz (f)	Intercept & slope of $\sigma_{ij}$ against $w_i$ equations		Dimensionless parameter		Estimated dipole moments in Coulomb metre		Reported $\mu$ 's in Coulomb metre	Estimated $\mu_1 \times 10^{30}$ in Coulomb metre from $\mu_1 = \mu_2 \times (c_1/c_2)^{1/2}$	$\mu_{theo} \times 10^{30}$ in Coulomb metre
		$\alpha \times 10^{-10}$	$\beta \times 10^{-10}$	$b_1$	$b_2$	$\mu_2 \times 10^{30}$	$\mu_1 \times 10^{30}$			
(I) chloral in benzene $M_j = 0.1475$ kg.	(a) 4.2	5.9901	4.2083	—	0.9810	5.0171	—	5.01*		
	(b) 9.8	13.7910	10.8002	0.9769	0.0727	19.3218	5.2729	4.87**	13.26	10.02
	(c) 24.6	34.8796	26.0102	—	0.8746	5.4584	—	5.28*		
(II) chloral in in n-Heptane	(a) 4.2	5.0582	3.6190	—	0.9798	5.7769	—	5.72*		
	(b) 9.8	11.7718	6.0011	0.9958	0.2824	9.0715	4.8308	6.00**	9.71	10.02
	(c) 24.6	29.6307	16.5130	0.9888	0.2714	9.6876	5.0757	5.10*	6.63	
(III) ethyl trichloroacetate in benzene $M_j = 0.1915$ Kg.	(a) 4.2	5.9896	9.0572	—	0.8028	9.2707	—	9.72*		
	(b) 9.8	14.0999	10.3344	—	0.2751	11.0739	—	6.50**		10.5
	(c) 24.6	34.1879	39.3565	—	0.5476	9.6681	—	8.05*		
(IV) ethyl trichloroacetate in n-hexane	(a) 4.2	4.9842	5.5989	—	0.8426	8.9744	—	8.99*		
	(b) 9.8	11.5334	12.7222	0.9986	0.3132	14.5260	8.1347	8.67**	17.15	10.5
	(c) 24.6	28.1599	36.5249	0.6662	0.1612	21.6555	10.6516	11.64*	16.37	

\*\* Ref. [5] \* Computed from the conductivity

**Table - 3.** Fröhlich parameter  $A$ , relative contributions  $c_1$  and  $c_2$  due to  $\tau_1$  and  $\tau_2$ , theoretical values of  $x$  and  $y$  from Fröhlich's equations (16) and (17) and from fitting equations as shown in Figures 4 and 5 at  $w_j \rightarrow 0$  and symmetric and asymmetric distribution parameters  $\gamma$  and  $\delta$  for the five polar-nonpolar liquid mixtures at 30°C.

System with Sl. No.	Frequency in GHz (f)	Fröhlich parameter $A =$ $\ln(\tau_2/\tau_1)$	Theoretical values of $x$ and $y$ from equs. (16) & (17)		Theoretical values of $c_1$ and $c_2$		Estimated values of $x$ and $y$ at $w_j \rightarrow 0$		Estimated values of $c_1$ and $c_2$		Estimated values of $\gamma$ and $\delta$	
			$x$	$y$	$c_1$	$c_2$	$x$	$y$	$c_1$	$c_2$	$\gamma$	$\delta$
(I) chloral in benzene	(b) 9.8	3.14	0.587	0.364	0.52	1.10	0.362	0.228	0.32	0.69	0.42	0.38
(II) chloral in n-heptane	(b) 9.8	3.12	0.803	0.296	0.65	0.56	0.610	0.318	0.43	0.64	0.26	0.42
	(c) 24.6	2.73	0.763	0.336	0.60	0.61	0.671	0.287	0.54	0.52	0.29	0.35
(IV) ethyltrichlo roacetate in n-hexane	(b) 9.8	3.69	0.843	0.255	0.69	0.49	0.44	0.284	0.26	0.59	0.34	0.42
	(c) 24.6	1.17	0.394	0.463	0.42	0.73	-0.32	0.383	-1.07	2.41	-0.62	-

where  $\gamma$  and  $\delta$  are symmetric and asymmetric distribution parameters which are, however, related to symmetric and characteristic relaxation times  $\tau_s$  and  $\tau_{cs}$  respectively.

Separating the real and the imaginary parts from equation (18) we have

$$\gamma = \frac{2}{\pi} \tan^{-1} \left[ (1-x) \frac{x}{y} - y \right] \quad \dots\dots\dots (20)$$

where  $x = (k'_{ij} - k_{\infty ij}) / (k_{oij} - k_{\infty ij})$  and  $y = k''_{ij} / (k_{oij} - k_{\infty ij})$  are obtained at  $w_j \rightarrow 0$  from Figures 4 and 5 respectively.

Similarly,  $\delta$  can be calculated as :

$$\tan (\delta\phi) = \frac{y}{x} \quad \dots\dots\dots (21)$$

$$\text{and } \log (\cos\phi)^{1/\phi} = \frac{\log \frac{x}{\cos (\delta\phi)}}{\delta\phi} \quad \dots\dots\dots (22)$$

where  $\tan \phi = w\tau_{cs}$ . To get  $\delta$ , a theoretical curve of  $\log (\cos\phi)^{1/\phi}$  against  $\phi$  is drawn as seen in figure 6. Knowing  $\delta\phi$  from equation (21);  $\phi$  can be found out from curve of figure 6. With the known  $\phi$ ,  $\delta$  can be estimated.  $\gamma$  and  $\delta$  are entered in the 12th and 13th columns of Table 3.

### 3. RESULTS AND DISCUSSIONS

Figure 1 showed that chloral and ethyl trichloro-acetate in different solvents under 24.6, 9.8 and 4.2 GHz electric field frequencies at 30°C are linear with the fitted data of  $(k_{oij} - k'_{ij}) / (k'_{ij} - k_{\infty ij})$  against  $k''_{ij} / (k'_{ij} - k_{\infty ij})$  at different  $w_j$ . The linearity is expressed in terms of correlation coefficients 'r' in the range of -0.24 to 0.99 as seen in Table 1. The percentage of errors in terms of r's involved in regression technique were calculated and placed in Table 1. The estimated

values of  $\tau_2$  and  $\tau_1$  from intercepts and slopes of equation (7) are placed in the 7th and 8th columns of Table 1. Double relaxation phenomena are, however, observed for chloral in n-heptane and ethyl trichloroacetate in n-hexane at 9.8 and 24.6 GHz electric field and chloral in benzene at 9.8 GHz electric field. This observation reveals that the probability of showing double relaxation phenomena in aliphatic solvents at higher frequencies is maximum for the apparently rigid aliphatic polar molecules. Chloral in  $C_6H_6$  at 9.8 GHz is an exception probably due to the fact that the effective dispersive region [15] lies near 10 GHz electric field for this system.  $\tau_2$ 's for the rest seven systems showing single relaxation phenomena were also calculated assuming single broad Debye-like dispersion [8] in them. They are placed in the 11th column of Table 1. It is interesting to note that  $\tau_1$ 's for the five systems agree well with the measured  $\tau_s$  from equation (10) due to conductivity measurement. This fact shows that hf conductivity measurement always yields the average microscopic  $\tau$  whereas the double relaxation phenomena offer a better understanding of microscopic as well as macroscopic molecular  $\tau$  as observed elsewhere [9].  $\tau_2$  of Table 1 is higher at 9.8 GHz and decrease gradually both at 4.2 GHz and 24.6 GHz electric fields in different solvents. This type of behaviour is probably due to larger size of the rotating unit in the effective dispersive region of 9.8 GHz due to solute-solvent or solute-solute molecular associations which break up with the increase or decrease from nearly 10 GHz electric field frequency. All the  $\tau_s$  and  $\tau_1$  agree well with the available reported  $\tau$  placed in the 10th column of Table 1 exhibiting the fact that the probability of rotation of a part of the molecule is possible under hf electric field [16].

The dipole moments  $\mu_2$  and  $\mu_1$  of the polar molecules were calculated in terms of dimensionless parameter  $b$ 's of equation (15) and slope  $\beta$  of  $(\sigma_{ij} - w_j)$  curve of Figure 2 as seen in Table 2.  $\mu_2$ 's are found to increase from 4.2 GHz to 24.6 GHz electric fields for chloral in n-heptane and ethyl trichloroacetate in n-hexane. This type of behaviour is probably due to rupture of solute-solute and solute-

solvent association in the hf electric field and the corresponding increase in the absorption for smaller molecular species [17]. But chloral and ethyl trichloroacetate in benzene show higher values of  $\mu_2$  at 9.8 GHz and decrease gradually from 24.6 GHz to 4.2 GHz electric field. Such type of behaviour may be due to strong absorption of electric energy at 9.8 GHz and solute-solvent association of the polar solute with benzene ring.  $\mu_2$  and  $\mu_1$  are, however, compared with the  $\mu_{\text{theo}}$ 's due to available bond angles and bond moments  $8.0 \times 10^{-30}$ ,  $5.0 \times 10^{-30}$ ,  $0.3 \times 10^{-30}$  and  $2.4 \times 10^{-30}$  Coulomb-metre for  $\text{C}=\text{O}$ ,  $\text{C}-\text{Cl}$ ,  $\text{C}-\text{C}$  and  $\text{C}-\text{OCH}_3$  (making an angle  $57^\circ$  with bond axis) respectively as displayed in Figure 3.  $\mu_{\text{theo}}$ 's are placed in the 11th column of Table 2. The molecule chloral shows slightly larger  $\mu_{\text{theo}}$  probably due to solute-solute molecular associations [Figure 3 (ii)] in the comparatively concentrated solution as expected. The solute-solute association may arise due to interaction of fractional positive charge  $\delta^+$  on C atom and negative charge  $\delta^-$  on O atom of  $\text{C}=\text{O}$  group between two solute molecules. The solute-solvent association with benzene is explained on the basis of the interaction between C atom of carbonyl group and  $\pi$ -delocalised electron cloud of benzene ring. Ethyl trichloroacetate, on the other hand, shows  $\mu_{\text{theo}}$  in agreement with the estimated  $\mu$ 's in  $\text{C}_6\text{H}_6$ . This is due to solute-solvent association as sketched in Figure (i) and (iii). Larger values of measured  $\mu$ 's are explained by the solute-solute interactions in solvent n-hexane due to interaction between adjacent C and O atoms of  $\text{C}=\text{O}$  groups of molecules as shown in Figure 3 (iv). However, the reduced bond moments by  $\mu_{\text{expt}}/\mu_{\text{theo}}$ 's in agreement with the estimated  $\mu$ 's indicates the presence of mesomeric and inductive effects in the polar groups of the molecules under consideration.

The relative contributions  $c_1$  and  $c_2$  towards dielectric dispersions due to  $\tau_1$  and  $\tau_2$  are however, calculated from  $x = (k'_{ij} - k_{\infty ij}) / (k_{0ij} - k_{\infty ij})$  and  $y = k''_{ij} / (k_{0ij} - k_{\infty ij})$  of equations (16) and (17) of Fröhlich's methods (11). They are compared with those due to  $x$  and  $y$  from graphical methods of Figures 4 and 5 at  $w_j \rightarrow 0$ . Both the methods yield  $c_1 + c_2 \simeq 1$  suggesting the applicability of the methods. The

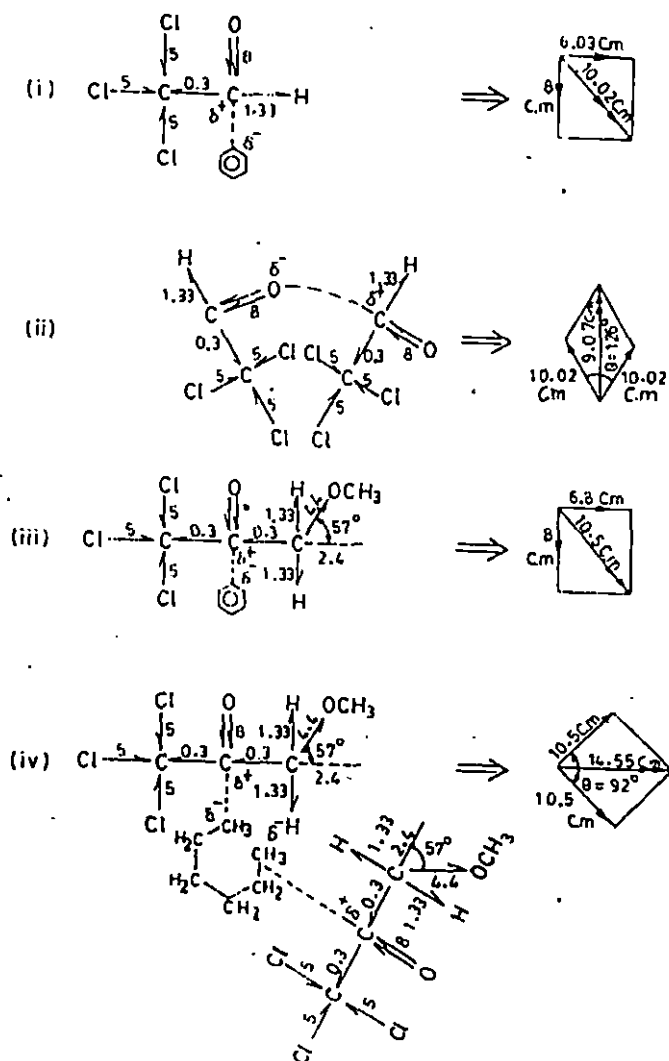


**Figure 3.** Conformational structures of chloral and ethyltrichloroacetate from bond angles and bond moments in multiple of  $10^{-30}$  Coulomb-metre. (i) Solute-solvent association of chloral in benzene, (ii) Solute-solute association of chloral; (iii) Solute-solvent association of ethyltrichloroacetate in benzene and (v) Solute-solute association of ethyltrichloroacetate in n-hexane.

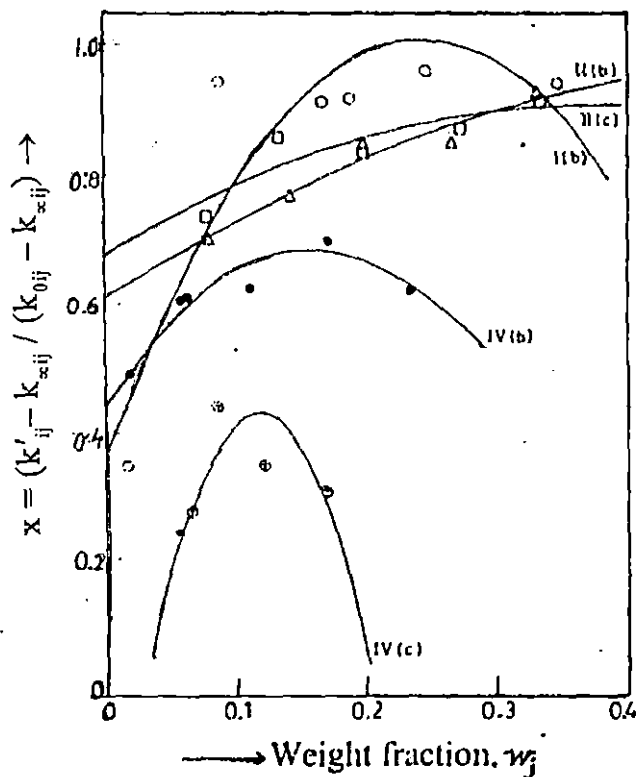


**Figure 4.** Variation of  $x = (k'_{ij} - k_{\infty ij}) / (k_{0ij} - k_{\infty ij})$  against different  $w_j$ 's of chloral and ethyltrichloroacetate at 30°C under various frequencies of GHz range I(b) for chloral in benzene at 9.8 GHz (O), II(b) and II(c) for chloral in n-heptane at 9.8 and 24.6 GHz ( $\Delta$ ,  $\square$ ); IV(b) and IV(c) for ethyltrichloroacetate in n-hexane at 9.8 and 24.6 GHz. ( $\bullet$ ,  $\oplus$ ).

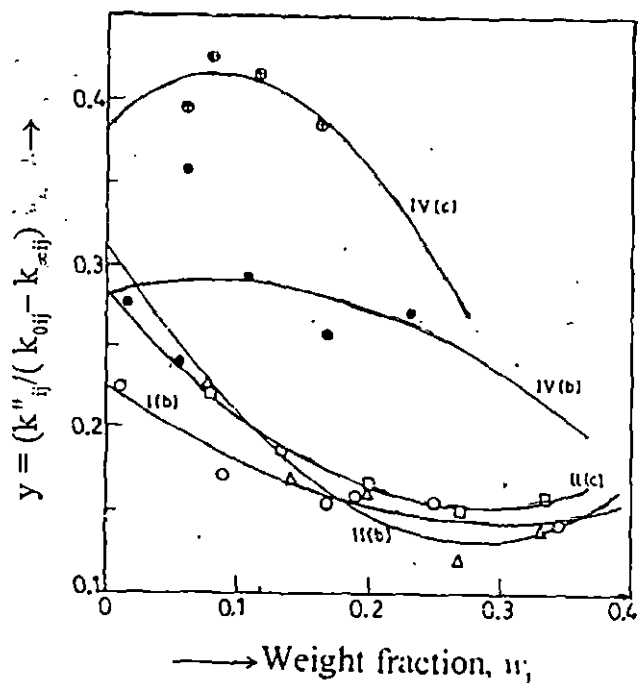


**Figure 5.** Variation of  $y = (k''_{ij} - k_{\infty ij}) / (k_{0ij} - k_{\infty ij})$  against different  $w_j$ 's of chloral and ethyltrichloroacetate at 30°C under various frequencies of GHz range I(b) for chloral in benzene at 9.8 GHz (O); II(b) and II(c) for chloral in n-heptane at 9.8 and 24.6 GHz ( $\Delta$ ,  $\square$ ); IV(b) and IV(c) for ethyltrichloroacetate in n-hexane at 9.8 and 24.6 GHz ( $\bullet$ ,  $\oplus$ ).

nature of variation of  $x$  and  $y$  with  $w_j$  is convex and concave (except ethyl trichloroacetate in  $n$ -hexane at 9.8 and 24.6 GHz which is not usual as observed earlier [7-9]). Such type of behaviour is explained on the basis of the fact that unlike increase of  $\tau$  [18] it decreases with  $w_j$  probably due to solute-solute and solute-solvent molecular association. All the values of  $c_1$  and  $c_2$  are placed in Table 3 for comparison. In order to test the rigidity of the molecules the symmetric and asymmetric distribution parameters  $\gamma$  and  $\delta$  were estimated from equations (20) and (21) for fixed values of  $x$  and  $y$  at  $w_j \rightarrow 0$  of Figures 4 and 5. The values of  $\log(\cos\phi)^{1/\phi}$  against  $\phi$  in degree as shown in Figure 6, is essential to get  $\delta$ . Knowing  $\phi$  from the curve of Figure 6;  $\delta$ 's were obtained. Both  $\gamma$  and  $\delta$  are placed in Table 3. The values  $\gamma$  establish the fact that the molecules obey the symmetric relaxation phenomena as  $\delta$ 's are very low [19].

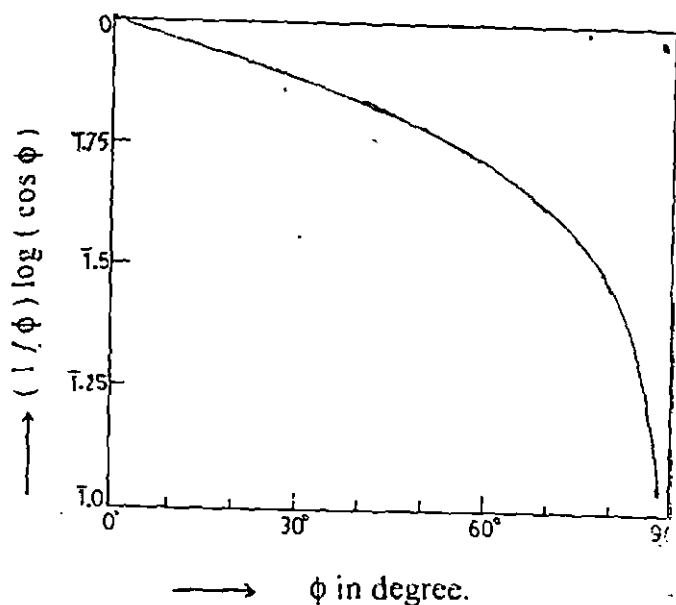


Figure 6 : Plot of  $(1/\phi) \log(\cos \phi)$  against  $\phi$  in degree.

#### 4. CONCLUSION

The study of dielectric relaxation mechanism by dimensionless dielectric constants gives a new insight of hf polar-polar and polar-nonpolar molecular interactions in a solution. The single frequency measurement of dielectric relaxation parameters provides a unique method to get macroscopic and microscopic relaxation times  $\tau_2$  and  $\tau_1$  and hence dipole moments  $\mu_2$  and  $\mu_1$  of the whole and the flexible part of the molecule. The estimation of  $\tau$  from a linear equation is very simple and straightforward to get  $\mu$  in terms of slope of  $\sigma_{ij} - w_j$  curve. The error in measurement can easily be computed by correlation coefficient. The molecules under different states of environment show interesting phenomena of double or single relaxation mechanism. The probability of showing double relaxation is, however, greater in nonpolar aliphatic solvents in hf region. Various types of molecular associations like solute-solute and solute-solvent interactions are thus inferred from departure of the graphical plots of  $x = (k'_{ij} - k_{\infty ij}) / (k_{oij} - k_{\infty ij})$  and  $y = k''_{ij} / (k_{oij} - k_{\infty ij})$  with  $w_j$  form Bergmann's equation. Nonrigid characteristics of the molecules are confirmed by estimation of symmetric  $\gamma$  and asymmetric distribution parameter  $\delta$  of them. The molecular associations are also supported by the conformational structures of the molecules in which the presence of mesomeric and inductive moments are found to play their role.

#### References

1. A.K. Sharma, D.R. Sharma and D.S. Gill, J.Phys. D : Appl. Phys **18** (1985) 1199.
2. A.. Sharma and D.R. Sharma, J. Phys. Soc. Japan **61** (1992) 1049.
3. K.S. Cole and R. H. Cole, J. Chem Phys. **9** (1941) 341.
4. D.W. Davidson and R.H. Cole, J. Chem Phys **19** (1951) 1484.
5. K. V. Gopalakrishna, Trans. Faraday Soc. **53** (1957) 767.
6. S. K. Srivastava and S.L. Srivastava, Indian J. Pure Appl. Phys. **13** (1975) 179.

7. U. Saha, S.K. Sit, R.C. Basak and S. Acharyya, *J. Phys. D : Appl. Phys.* **27** (1994) 596.
8. S. K. Sit, R.C. Basak, U. Saha and S. Acharyya, *J. Phys. D : Appl. Phys.* **27** (1994) 2194.
9. S. K. Sit and S. Acharyya, *Indian J. Phys.* **70B** (1996) 19.
10. S. K. Sit, N. Ghosh and S. Acharyya, *Indian J. Pure Appl. Phys.* **35** (1997) 329.
11. H. Fröhlich, *Theory of Dielectrics* (Oxford : Oxford University Press) (1949) P. 94.
12. K. Bergmann, D. M. Roberti and C.P. Smyth, *J. Phys. Chem.* **64** (1960) 665.
13. C.P. Smyth, *Dielectric Behaviour and Structure* (New York : McGraw Hill) (1955).
14. R. C. Basak, A. Karmakar, S.K. Sit and S. Acharyya, *Indian J. Pure Appl. Phys.* **37** (1999) 224.
15. S. K. Sit and S. Acharyya, *Indian J. Pure Appl. Phys.* **34** (1996) 225.
16. R.C. Basak, S. K. Sit, N. Nandi and S. Acharyya, *Indian J. Phys.* **70B** (1996) 37.
17. L. Glasser, J. Crossley and C.P. Smyth, *J. Chem. Phys.* **57** (1972) 3977.
18. S.N. Sen and R. Ghosh, *Indian J. Pure Appl. Phys.* **10** (1972) 701.
19. S. Chandra and J. Prakash, *J. Phys. Soc. Japan* **35** (1975) 876.